Thermal quantum transition-path-time distributions, time averages, and quantum tunneling times

Eli Pollak*

Chemical Physics Department, Weizmann Institute of Science, 76100 Rehovoth, Israel

(Received 25 January 2017; published 10 April 2017)

The transition-path-time distribution is formalized for quantum systems and applied to a number of examples. Using a symmetrized thermal density, transition times are studied for the free particle, a δ-function potential, a square-barrier potential, and symmetric-double-well dynamics at very low temperature. These studies exemplify extreme nonlocality for motion in δ-function potentials, vanishing tunneling times for the square-barrier potential, and varying transit times in the symmetric-double-well potential. In all cases, there are regions where the longer the distance traversed, the shorter the mean transit time is. For the thermal density correlation functions studied here, the Hartman effect exemplifies itself through the independence of the transit time on the barrier height. However, due to the thermal distribution, the transit time does depend on the barrier width, initially decreasing with increasing width but then increasing again.

DOI: 10.1103/PhysRevA.95.042108

I. INTRODUCTION

Time has been an enigma in quantum mechanics from the very beginning [1]. In contrast to the noncommuting momentum coordinate operators, it is much more difficult to construct conjugate time energy operators. The difficulties stem from many factors, not least among them being the quasiobjection by Pauli [2], which stated that if there would be such a pair of canonically conjugate self-adjoint operators, then necessarily the energy operator would have to be unbounded from below. Some of the history of the evolution in the construction of time operators in quantum mechanics may be found in the introductory chapter by Muga *et al.* [3] to two recent volumes [4,5] summarizing many of the complexities involved in the definition of a time operator in quantum mechanics. Since then, additional reviews have appeared [6–12] as well as different suggestions for time operators [13,14].

Arguably, the operator approach has not resolved some fundamental questions such as how much time does it take a quantum system to tunnel through a barrier. Different definitions of the time operator give different answers to something that naively one would expect would have a unique answer [9,15]. The same comment holds when using external clocks to "measure" quantum time. Different clocks give different times [16].

There are many additional approaches to the time problem in quantum mechanics. One example is the quantum arrival time distribution, defined in terms of a time integral of the absolute value of the current density [17,18]. Another is known as the quantum presence time [19,20], where one considers the time average of the quantum density. This approach has been used to define a tempus operator [21]. Its relation to other definitions of quantum time has been studied in Ref. [22]. Sokolovski pioneered the use of Feynman's path integral to define quantum times [23,24] and related this approach to previous descriptions.

This present paper is motivated by the development in recent years of the transition-path-time distribution, used especially in the context of protein folding [25–29]. The transition-path-time distribution considers the probability that a transition between two points in space of a molecular system (typically a protein) will take a time t. Recent experiments of Neupane *et al.* have demonstrated that the distribution is measurable [30] and may be fit to a theoretical expression based on the Smoluchowski dynamics of a parabolic barrier. A central challenge is to provide a quantum-mechanical framework for the quantum transition-path-time distribution, paying special attention to the thermal density.

The classical transition-path-time distribution was originally formulated in terms of thermal flux time correlation functions [25–29]. This suggests a formal generalization of transition-path times in terms of more general time correlation functions. The paradigm we will thus use here is that one should consider the quantum-mechanical time in terms of quantum time correlation functions [31,32]. In the Heisenberg picture, operators evolve in time t; in the Schrödinger picture wave functions evolve in time. In both cases, the central object is the propagator $\exp(-i\hat{H}t/\hbar)$ (the caret denotes operators and $\hat{H}$ is the Hamiltonian operator). By studying time correlation functions (say, of $\hat{A}$ at $t = 0$ with $\hat{B}$ at time t), one obtains information on the time development of the system with property $\hat{B}$ from its initial property $\hat{A}$. If the correlation function is positive, then it can be used to make a statement on the probability of finding the system at time t with property $\hat{B}$. The presence time formalism [19,20] is just one specific case of such a correlation function.

With this correlation function approach, one does not need to formulate a time operator. It is clear that for different correlation functions one can and will obtain different time distributions. They simply reflect the different experiments needed to measure the differing correlation functions. Given though an experiment, or equivalently a correlation function, one may establish mean transit times. A study of the mean transit time for different correlation functions may reveal the underlying dynamics and may give a unique answer to questions such as how long it takes a particle to tunnel through a barrier.

The theoretical framework for quantum transition-path-time distributions is presented in Sec. II. Following a suggestion of Ref. [33], a relation between thermal correlation functions at temperature T using a symmetric breakup of the

*eli.pollak@weizmann.ac.il

thermal distribution of the form $\exp(-\beta\hat{H}/2)\hat{\rho}\exp(-\beta\hat{H}/2)$ (with $\beta = 1/k_BT$ and $\hat{\rho}$ the density operator) and the standard thermal correlation functions is worked out. There is a direct relation between the Fourier transforms of the two correlation functions, so measurement of the standard correlation function implies the determination of the correlation function with the symmetric form of the thermal density distribution. The advantage of the symmetric form is that it leads to a positive transition-path-time probability distribution.

The thermal density transition-time correlation function is then studied for a few systems, for which the quantum propagator is known analytically. These include the free particle, the δ-function potential [34], the square-barrier potential [35,36], and the symmetric-double-well potential at very low temperature. These studies reveal some interesting properties. For example, for the free particle, the time integral of the thermal density correlation function diverges both classically and quantum mechanically. Yet when considering a δ-function barrier or well, even arbitrarily far from the δ-function center, the time integral of the quantum thermal density correlation function does not diverge. The quantum particle experiences the potential at an infinite distance. This allows for the determination of the average transit time. As noted in a recent paper for the parabolic barrier [31], here too (and also for the square barrier) there are regions where the longer the path taken by the quantum system, the shorter the mean time it takes to get there.

The analysis of the square-barrier thermal density correlation function is also revealing. For a fixed barrier width, the tunneling time is found to be independent of the square-barrier height. However, keeping the barrier height fixed and increasing the width does not give a mean transit time that is independent of the barrier width. The well-known Hartman effect [37–39], which says that the tunneling time becomes independent of the barrier width, is not what one would observe experimentally when initially the particle density on one side of the barrier is thermally distributed. When the barrier width becomes large enough such that the tunneling probability becomes less than the Boltzmann factor for above barrier motion, the Boltzmann factor takes over, the major contribution to the barrier traversal comes from above barrier energies, and the barrier transit time increases with a further increase in the barrier width. This is qualitatively similar to the same effect found for an incident Gaussian wave packet [19].

The last example considered is a symmetric-double-well potential at very low energies [40] such that only the lowest tunneling doublet is populated. The well-known tunneling time ($\tau \sim 2\pi\hbar/\Delta E$) as obtained from the energy splitting ΔE of the doublet only sets the overall time scale for the transit time obtained from the thermal density correlation function. The actual transit time depends on the location at which one measures it and is a continuous function of the location.

The paper ends with a discussion of the results, noting that the cases considered here in some detail are just the beginning of the discussion. For example, one may replace the initial thermal distribution and the final density operator with projection operators onto coherent states. One may use the correlation function transit-time approach to consider the time characteristics of almost any quantum transition.

II. THERMAL TRANSITION-PATH-TIME PROBABILITY DISTRIBUTION

A. Introduction

For the sake of simplicity, the formalism will be written out for a one-dimensional system; generalization to the multidimensional case is straightforward. We assume that the system is governed by the Hamiltonian operator for a particle with mass M:

$$\hat{H} = \frac{\hat{p}^2}{2M} + V(\hat{q}), \tag{2.1}$$

where $\hat{p}$ and $\hat{q}$ are the momentum and coordinate operators, respectively, and $V(\hat{q})$ is the potential operator. The details of the potential are as of yet unimportant. The transition path involves motion from a point x to a point y occurring in the time interval t. We specifically assume a thermal distribution. The time-dependent density operator is

$$\hat{\rho}(y,t) = \exp\left(\frac{i\hat{H}t}{\hbar}\right)\delta(\hat{q}-y)\exp\left(-\frac{i\hat{H}t}{\hbar}\right). \tag{2.2}$$

The thermal transition-path-time correlation function is then defined as

$$C(t;x,y) = \tfrac{1}{2}\mathrm{Tr}\{[\exp(-\beta\hat{H})\delta(\hat{q}-x) + \delta(\hat{q}-x)\exp(-\beta\hat{H})]\hat{\rho}(y,t)\}. \tag{2.3}$$

This is the standard symmetrized definition of thermal correlations functions. Normalization will be introduced below. We also define the Fourier transform (using a tilde)

$$\tilde{C}(\omega;x,y) = \frac{1}{2\pi}\int_{-\infty}^{\infty} dt\,\exp(-i\omega t)C(t;x,y). \tag{2.4}$$

In practice we will consider a different symmetrized thermal density

$$\hat{\rho}(x,\beta) = \exp\left(-\frac{\beta\hat{H}}{2}\right)\delta(\hat{q}-x)\exp\left(-\frac{\beta\hat{H}}{2}\right) \tag{2.5}$$

and the related correlation function

$$C_s(t;x,y) = \mathrm{Tr}[\hat{\rho}(x,\beta)\hat{\rho}(y,t)]. \tag{2.6}$$

Following Craig and Manolopoulos [33], using the eigenfunction basis set, one readily finds that

$$\tilde{C}_s(\omega;x,y) = \frac{\tilde{C}(\omega;x,y)}{\cosh(\frac{\beta\hbar\omega}{2})}. \tag{2.7}$$

This implies that measurement of the physical correlation function $C(t;x,y)$ will yield, via its Fourier transform, also the symmetrized correlation function $C_s(t;x,y)$, so one may use either one of the correlation functions to study the quantum dynamics. The advantage of working with the symmetrized correlation function is that it is positive:

$$C_s(t;x,y) = \left|\left\langle x\left|\exp\left(-i\frac{\hat{H}t_c}{\hbar}\right)\right|y\right\rangle\right|^2 \tag{2.8}$$

with

$$t_c = t - i\frac{\hbar\beta}{2}. \tag{2.9}$$

B. Time-integrated density operator

It is instructive to derive the relation between the standard and symmetrized correlation functions somewhat differently. The time-integrated density operator at the point y is by definition

$$\hat{D}_0(y) = \int_{-\infty}^{\infty} dt\, \hat{\rho}(y,t). \tag{2.10}$$

Following Ref. [41], we note that the time-integrated density operator commutes with the Hamiltonian

$$\begin{aligned}
&\hat{D}_0(y)\exp(-\beta\hat{H}) \\
&= \int_{-\infty}^{\infty} dt \exp\left(\frac{i\hat{H}t}{\hbar}\right)\delta(\hat{q}-y)\exp\left(-\frac{i\hat{H}(t-i\hbar\beta)}{\hbar}\right) \\
&= \int_{-\infty}^{\infty} dt \exp\left(\frac{i\hat{H}(t+i\hbar\beta)}{\hbar}\right)\delta(\hat{q}-y)\exp\left(-\frac{i\hat{H}t}{\hbar}\right) \\
&= \exp(-\beta\hat{H})\hat{D}_0(y).
\end{aligned} \tag{2.11}$$

The second equality follows from changing the variable of integration from t to $t - i\hbar\beta$ and the fact that the time interval of integration goes from $-\infty$ to ∞. This commutativity is of course not restricted to the density operator; any Heisenberg evolved operator that is similarly time integrated will also commute with the Hamiltonian. This result implies that

$$\begin{aligned}
&\int_{-\infty}^{\infty} dt C(t;x,y) \\
&= \frac{1}{2}\mathrm{Tr}\{[\exp(-\beta\hat{H})\delta(\hat{q}-x)+\delta(\hat{q}-x)\exp(-\beta\hat{H})]\hat{D}_0(y)\} \\
&= \mathrm{Tr}\left[\exp\left(-\frac{\beta\hat{H}}{2}\right)\delta(\hat{q}-x)\exp\left(-\frac{\beta\hat{H}}{2}\right)\right]\hat{D}_0(y) \\
&= \int_{-\infty}^{\infty} dt C_s(t;x,y),
\end{aligned} \tag{2.12}$$

where the second equality is obtained by using the commutativity as in Eq. (2.11) and the invariance of the Tr operation to cyclic invariance. Of course, the same result is also obtained from Eq. (2.7) by using the equality for $\omega = 0$.

One may then define the time-averaged density operator

$$\hat{D}_1(y) = \int_{-\infty}^{\infty} dt\, t\hat{\rho}(y,t). \tag{2.13}$$

As for $\hat{D}_0(y)$, one readily finds that

$$\hat{D}_1(y)\exp(-\beta\hat{H}) = \exp(-\beta\hat{H})[\hat{D}_1(y) + i\hbar\beta\hat{D}_0(y)]. \tag{2.14}$$

C. Thermal quantum transition-path-time probability distribution

Following the same change of variables as in the derivation of Eq. (2.11) and using the invariance of the Tr operation to cyclic permutation we find

$$\begin{aligned}
\int_{-\infty}^{\infty} dt\, tC(t;x,y) = \mathrm{Tr}\Bigg[&\exp\left(-\frac{\beta\hat{H}}{2}\right)\delta(\hat{q}-x) \\
&\times \exp\left(-\frac{\beta\hat{H}}{2}\right)\hat{D}_1(y)\Bigg],
\end{aligned} \tag{2.15}$$

demonstrating that also the first moment of the two correlation functions $C(t;x,y)$ and $C_s(t;x,y)$ are identical. The same result may also be obtained from Eq. (2.7) by taking the first derivative with respect to ω and then setting $\omega = 0$.

We may thus define a normalized quantum transition-path-time probability distribution function

$$P(t;x,y) = \frac{C_s(t;x,y)}{\int_{-\infty}^{\infty} dt C_s(t;x,y)}, \tag{2.16}$$

whose first moment is identical to the normalized time average of the original correlation function $C(t;x,y)$. The advantage is that in view of Eq. (2.8), now we have a true probability distribution, which is always positive; this is not the case when considering $C(t;x,y)$.

Following the same procedure as above, one may also define the second moment of the integrated density operator

$$\hat{D}_2(y) = \int_{-\infty}^{\infty} dt t^2 \hat{\rho}(y,t) \tag{2.17}$$

and find that

$$\int_{-\infty}^{\infty} dt t^2 C(t;x,y) = \mathrm{Tr}\left[\hat{\rho}(x,\beta)\left(\hat{D}_2(y) - \frac{\hbar^2\beta^2}{4}\hat{D}_0(y)\right)\right]. \tag{2.18}$$

The same result may also be obtained directly from Eq. (2.7) by taking the second derivative of the equation with respect to ω and then setting $\omega = 0$. This implies that

$$\int_{-\infty}^{\infty} dt t^2 P(t;x,y) = \frac{\int_{-\infty}^{\infty} dt t^2 C(t;x,y)}{\int_{-\infty}^{\infty} dt C(t;x,y)} + \frac{\hbar^2\beta^2}{4}. \tag{2.19}$$

Since often the probability function $P(t;x,y)$ is symmetric with respect to time inversion, it is also useful to note the relationship

$$\int_{-\infty}^{\infty} dt|t|P(t;x,y) = \frac{\int_{-\infty}^{\infty} dt\sqrt{t^2 + \frac{\hbar^2\beta^2}{4}}C(t;x,y)}{\int_{-\infty}^{\infty} dt C(t;x,y)}. \tag{2.20}$$

Below we will study in some detail the properties of the mean transition-path time defined as

$$\langle t;x,y\rangle = \int_{-\infty}^{\infty} dt|t|P(t;x,y). \tag{2.21}$$

It should be stressed that, by using the symmetrized correlation function, one gets a positive distribution for which one can legitimately consider moments and these moments have a straightforward physical meaning. The time-dependent transition-path probability is the probability that a particle localized initially at x with a thermal distribution will end up at the point y at time t. In this way one has a direct handle on the passage of time in quantum mechanics. There is no further need to define time operators or worry about the lack of a well-defined conjugate energy operator. Time in this formalism is just the time that elapsed between two successive localizations of the quantum system.

D. Dwell-time operator

It is of interest to compare the average time as obtained from the thermal transition-path-time probability distribution (2.20) with one of the more standard definitions of time in quantum mechanics. The dwell-time operator in the region $[a,b]$ as defined, for example, in Ref. [3] is the spatially integrated form of the time-integrated density operator

$$\hat{T}(a,b) = \int_a^b dy \hat{D}_0(y). \tag{2.22}$$

The thermally averaged dwell time in the region $[a,b]$,

$$\langle \hat{T}(a,b)\rangle_\beta = \frac{\mathrm{Tr}[\exp(-\beta\hat{H})\hat{T}(a,b)]}{\mathrm{Tr}[\exp(-\beta\hat{H})]}, \tag{2.23}$$

is not meaningful since the time integral in the numerator always diverges. It is instructive though to study a conditional thermal dwell time

$$\begin{aligned}\langle \hat{T}(x;a,b)\rangle_\beta &= \frac{\mathrm{Tr}[\exp(-\beta\hat{H})\delta(\hat{q}-x)\hat{T}(a,b)]}{\mathrm{Tr}[\exp(-\beta\hat{H})\delta(\hat{q}-x)]} \\ &= \frac{\int_a^b dy \int_{-\infty}^{\infty} dt \left|\langle x| \exp\left(-i\frac{\hat{H}t_c}{\hbar}\right)|y\rangle\right|^2}{\langle x|\exp(-\beta\hat{H})|x\rangle},\end{aligned} \tag{2.24}$$

which gives the dwell time in the interval $[a,b]$ conditioned about the thermal distribution being initially localized at x.

E. Generalizations

To consider the quantum-mechanical time evolution in terms of a transition-path-time probability function it is not necessary to limit oneself to thermal density distributions. As noted in Ref. [31], the correlation function of the operators $\hat{A}$ and $\hat{B}$,

$$C_{AB}(t) = \mathrm{Tr}\left[\hat{A}\exp\left(\frac{i\hat{H}t}{\hbar}\right)\hat{B}\exp\left(-\frac{i\hat{H}t}{\hbar}\right)\right], \tag{2.25}$$

is positive for any time if the two operators may be represented as

$$\hat{A} = \hat{a}\hat{a}^\dagger, \quad \hat{B} = \hat{b}\hat{b}^\dagger \tag{2.26}$$

since then the correlation function is just the trace of a product of an operator and its Hermitian conjugate. This is especially relevant when the operators $\hat{A}$ and $\hat{B}$ are projection operators. For example, one may choose

$$\hat{A} = |g(p,q)\rangle\langle g(p,q)|, \quad \hat{B} = |g(p',q')\rangle\langle g(p',q')|, \tag{2.27}$$

where $|g(p,q)\rangle$ is a coherent state localized about the coordinate and momentum values q and p, respectively. Alternatively, one may choose the operator $\hat{B}$ to be the density at the point y and then one obtains the presence time distribution for the initial coherent state.

III. APPLICATIONS

A. Free particle

In this section we will study a few systems whose propagator is known analytically using the transition-path-time probability distribution. The propagator matrix element for a free particle is [42]

$$\langle x|\exp\left(-\frac{i\hat{H}t}{\hbar}\right)|y\rangle = \sqrt{\frac{-iM}{2\pi\hbar t}}\exp\left[\frac{iM(x-y)^2}{2\hbar t}\right], \tag{3.1}$$

so

$$C_s(t;x,y) = \frac{M}{2\pi\hbar}\sqrt{\frac{1}{t^2+\frac{\hbar^2\beta^2}{4}}}\exp\left[-\frac{M\beta(x-y)^2}{2\left(t^2+\frac{\hbar^2\beta^2}{4}\right)}\right]. \tag{3.2}$$

The infinite time integral of the free-particle thermal transition-path-time correlation function diverges logarithmically at long times. This divergence is a classical effect, as one notes when letting $\hbar \to 0$ in Eq. (3.2). The classical time it takes to traverse the distance $|x-y|$ is inversely proportional to the momentum and diverges as the momentum goes to zero, so the related probability distribution is not well defined. The conditional thermal dwell time in the region $[a,b]$ [Eq. (2.17)] for a free particle is similarly not well defined.

It is also of interest to consider the Wigner distribution associated with the density $\hat{\rho}(x,\beta)$ [Eq. (2.5)]:

$$\begin{aligned}&\rho_W(p,q;x,\beta) \\ &= \frac{1}{2\pi\hbar}\int_{-\infty}^{\infty} d\xi \exp\left(\frac{ip\xi}{\hbar}\right)\left\langle q-\frac{\xi}{2}\right|\exp\left(-\frac{\beta\hat{p}^2}{4M}\right)\delta(\hat{q}-x) \\ &\quad\times\exp\left(-\frac{\beta\hat{p}^2}{4M}\right)\left|q+\frac{\xi}{2}\right\rangle \\ &= \frac{1}{\pi\hbar}\left(\frac{M}{2\pi\hbar^2\beta}\right)^{1/2}\exp\left(-\frac{\beta p^2}{2M}-\frac{2M(x-q)^2}{\hbar^2\beta}\right).\end{aligned} \tag{3.3}$$

In the Wigner phase-space representation, the distribution is localized about the position x but with a width that is $\hbar\sqrt{\beta/4M}$, so the lower the temperature, the larger the width in the configuration space. This is of course expected; the lower the temperature, the more localized the momentum, so the coordinate delocalizes. As we will see below, this manifests itself when studying the transit time in the presence of a potential.

B. The δ-function potential

Following the notation of Ref. [34], we write the Hamiltonian as

$$\hat{H} = \frac{\hat{p}^2}{2M} - \varepsilon\delta(\hat{q}) \tag{3.4}$$

and note that for a barrier, $\varepsilon < 0$. The transmission (T) and reflection (R) coefficients for an energy

$$E = \frac{\hbar^2k^2}{2M} \tag{3.5}$$

and incident wave function

$$\Psi(q) = \exp(ikq) + R\exp(-ikq), \quad q < 0 \tag{3.6}$$

and transmitted wave function

$$\Psi(q) = T\exp(ikq), \quad q > 0 \tag{3.7}$$

are

$$T = \left(1 - i\frac{M\varepsilon}{k\hbar^2}\right)^{-1}, \quad R = \frac{i\frac{M\varepsilon}{k\hbar^2}}{1-i\frac{M\varepsilon}{k\hbar^2}}. \tag{3.8}$$

The transmission and reflection probabilities are thus quadratic in the variable ε; they do not distinguish between a δ-function well or barrier:

$$|T|^2 = \left(1 + \frac{M^2\varepsilon^2}{k^2\hbar^4}\right)^{-1},$$
$$|R|^2 = \frac{M^2\varepsilon^2}{k^2\hbar^4}\left(1 + \frac{M^2\varepsilon^2}{k^2\hbar^4}\right)^{-1}. \tag{3.9}$$

The matrix element for the propagator in imaginary time has been worked out in Ref. [34]. It too is invariant to the sign of ε:

$$\langle x|\exp(-\hat{H}\tau)|y\rangle = \sqrt{\frac{M}{2\pi\hbar^2\tau}}\left[\exp\left(-\frac{M(x-y)^2}{2\hbar^2\tau}\right) - \frac{M|\varepsilon|}{\hbar^2} \times \int_0^\infty du \exp\left(-\frac{M|\varepsilon|}{\hbar^2}u\right)\exp\left(-\frac{M(|x|+|y|+u)^2}{2\hbar^2\tau}\right)\right]. \tag{3.10}$$

Using the dimensionless variables

$$\bar{x} = \sqrt{\frac{M}{\beta\hbar^2}}x, \quad \bar{t} = \frac{t}{\beta\hbar}, \quad \bar{\varepsilon} = \frac{\varepsilon}{\hbar}\sqrt{M\beta}, \tag{3.11}$$

we find that

$$|\langle\bar{x}|\exp(-i\hat{H}t_c)|\bar{y}\rangle|^2 = \frac{1}{2\pi}\sqrt{\frac{1}{(\bar{t}^2+\frac{1}{4})}}\exp\left(-\frac{(\bar{x}-\bar{y})^2}{2(\bar{t}^2+\frac{1}{4})}\right) \times \left|1 + \bar{\varepsilon}\sqrt{\frac{i\pi\bar{t}_c}{2}}\exp\left\{\frac{i}{2}\left[\bar{\varepsilon}^2\left(\bar{t}_c - 2\frac{i(|\bar{x}|+|\bar{y}|)}{|\bar{\varepsilon}|}\right) - \frac{(\bar{x}-\bar{y})^2}{\bar{t}_c}\right]\right\}\mathrm{erfc}\left(\frac{|\bar{x}|+|\bar{y}|+i\bar{t}_c|\bar{\varepsilon}|}{\sqrt{2i\bar{t}_c}}\right)\right|^2. \tag{3.12}$$

In contrast to the free particle, this expression does not have a logarithmic divergence at long times. To see this we note the leading terms in the asymptotic expansion

$$\mathrm{erfc}(z) \sim \frac{1}{\sqrt{\pi}z}\exp(-z^2)\left(1 - \frac{1}{2z^2}\right) \tag{3.13}$$

so that

$$\lim_{t\to\infty}|\langle\bar{x}|\exp(-i\hat{H}t_c)|\bar{y}\rangle|^2 = \frac{1}{2\pi}\sqrt{\frac{1}{\bar{t}^2+\frac{1}{4}}}\frac{[1+\bar{\varepsilon}^2(|\bar{x}||\bar{y}|+\bar{x}\bar{y})+|\bar{\varepsilon}|(|\bar{x}|+|\bar{y}|)]^2}{(\bar{t}^2+\frac{1}{4})\bar{\varepsilon}^4}. \tag{3.14}$$

This is integrable irrespective of the sign of $\bar{\varepsilon}$. The mean time also does not diverge. This is one of the peculiarities of quantum mechanics. One may have thought that very far away from the origin, the transmitted wave function is just a free particle. However, this is not so; at any distance, the particle experiences the δ-function potential and the time-integrated normalization of the thermal correlation function does not diverge as it does for a free particle.

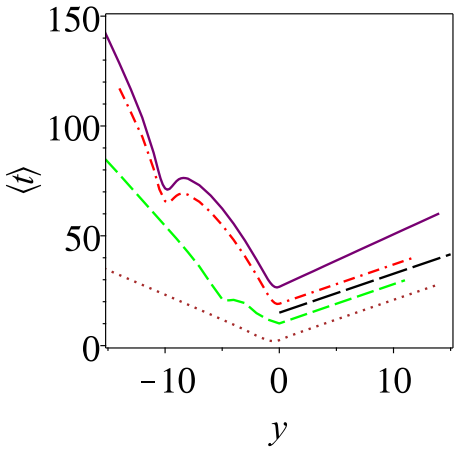

FIG. 1. Mean (reduced) transition-path time for a δ-function potential for different initial points of the particle plotted as a function of the reduced final position y. The red dash-dotted, green dashed, and brown dotted lines are $\bar{x} = -10, -5, -1$, respectively, with $|\bar{\varepsilon}| = 1$. The lower black long-dashed line shows a linear dependence with slope of $\sqrt{\pi}$. The solid purple line shows the dependence of the average transit time for $|\bar{\varepsilon}| = 0.5$ and $\bar{x} = -10$. Note the regions in which the average time decreases as the distance from the initial point increases.

In Fig. 1 we plot the average transit time for the δ-function potential for three different initial points $\bar{x} = -10, -5, -1$ as the red dash-dotted, green dashed, and brown dotted lines, respectively, as a function of the final point $\bar{y}$ for $|\bar{\varepsilon}| = 1$. These plots have some notable features. For positive $\bar{y}$, that is, for points on the opposite side of the δ-function potential, the average time increases linearly with the final position, as might be expected for a free particle. The slope is independent of the initial point $\bar{x}$ and is found empirically to be equal to $\sqrt{\pi}$ (the black long-dashed line in the figure). Between the initial point $\bar{x}$ and the location of the δ function ($\bar{x} = 0$) the average time decreases as the particle moves a longer distance. As noted in Ref. [31] for the parabolic barrier, in quantum mechanics, sometimes, going a longer way takes less time. In this case, this quantum effect is a manifestation of the interference of the incident and reflected waves in this region. For points on the left of the initial point, the time increases with increasing distance; this is a manifestation of the fact that the initial density includes both positive and negative momenta.

To demonstrate the dependence of the transition time on the magnitude of the strength of the δ potential we show in the same figure the dependence of the average time on the final point $\bar{y}$ also for $|\bar{\varepsilon}| = 0.5$ (brown solid line) with the initial condition $\bar{x} = -10$. When $\bar{\varepsilon} = 0$ the δ-function potential vanishes, one has a free particle, and the average transit time becomes infinite. One should thus expect that the transition time will increase as $\bar{\varepsilon}$ decreases, as shown in the figure.

Finally, it is of interest to compare the average transition-path time with the conditional dwell time as defined in Eq. (2.17). For this purpose we note that for the δ-function

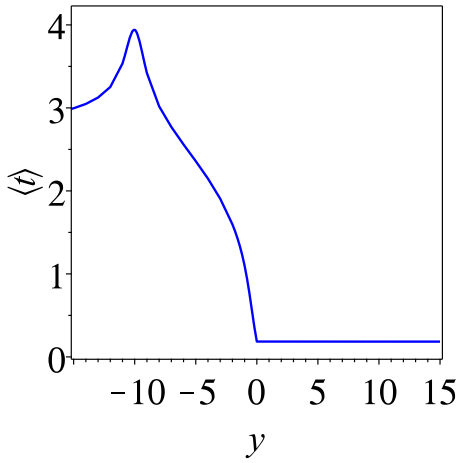

FIG. 2. Conditional dwell time for a δ-function potential plotted as a function of the final distance for boxes of reduced length of unity. The initial point is $\bar{x} = -10$ and $|\bar{\varepsilon}| = 1$. Note that to the right of the potential the conditional dwell time is constant and small, reflecting the small transition probability.

potential

$$\langle \bar{x}|\exp(-\beta\hat{H})|\bar{x}\rangle = \sqrt{\frac{1}{2\pi}}\left[1 - |\bar{\varepsilon}|\sqrt{\frac{\pi}{2}}\exp\left(\frac{1}{2}(\bar{\varepsilon}^2 + 4|\bar{x}||\bar{\varepsilon}|)\right) \times \mathrm{erfc}[\sqrt{2}(|\bar{\varepsilon}| + 2|\bar{x}|)]\right]. \quad (3.15)$$

The conditional dwell time is plotted in Fig. 2 for successive regions of length unity, that is, we plot $\langle \hat{T}(-10;\bar{y}-\frac{1}{2},\bar{y}+\frac{1}{2})\rangle_\beta$ for $|\bar{\varepsilon}| = 1$ as a function of $\bar{y}$. The conditional dwell time is very different from the mean transition-path time. To the right of the δ potential, it is very small, reflecting the small transmission probability. The discontinuity in the derivative of the dwell time about the origin is real and reflects the discontinuity in the derivative of the wave function due to the δ-function potential. In contrast, the average transition-path time does not reflect the small transition probability since it gives the physical time. That is, if one first localizes the particle to the right of the δ potential, it gives the time it will take it to reach the final point. The fact that the probability of reaching the point is small or large is irrelevant.

C. Square barrier potential

We follow here the notation of Ref. [36]. The step function barrier Hamiltonian is

$$\hat{H} = \frac{\hat{p}_q^2}{2M} + u_0[\theta(x+a) - \theta(x-a)], \quad (3.16)$$

so the barrier is of length $2a$ and height u_0. Region 1 is defined by $x < -a$, region 0 is the barrier region, that is, $a > x > -a$, and region 2 is when $x > a$. Using the notation of Eq. (3.5) for the wave number k and

$$K = \sqrt{\frac{2Mu_0}{\hbar^2} - k^2}, \quad (3.17)$$

the expression for the propagator as given in Ref. [36] is

$$\langle x|K_{ij}(t)|y\rangle = \int_0^\infty dk \exp\left(-i\frac{\hbar k^2}{2M}t\right) Z_{ij}(k,x,y), \quad (3.18)$$

where the index j denotes the region of y and the index i the region of x. The functions $Z_{ij}(k,x,y)$ are real and written out explicitly in the Appendix. For the thermal distribution the normalization integral is

$$N_{ij}^{-1}(x,y) = \int_{-\infty}^\infty dt|\langle x|K_{ij}(t_c)|y\rangle|^2 = \frac{2\pi M}{\hbar}\int_0^\infty dk\frac{1}{k}\exp\left(-\beta\frac{\hbar^2k^2}{2M}\right)|Z_{ij}(k,x,y)|^2 \quad (3.19)$$

and for the mean time integral

$$\int_{-\infty}^\infty dt|t||\langle x|K_{ij}(t_c)|y\rangle|^2 = 2\int_0^\infty dtt\left|\int_0^\infty dk\exp\left(-\beta\frac{\hbar^2k^2}{4M}\right) \times \cos\left(\frac{\hbar k^2}{2M}t\right)Z_{ij}(k,x,y)\right|^2 + 2\int_0^\infty dtt\left|\int_0^\infty dk\exp\left(-\beta\frac{\hbar^2k^2}{4M}\right) \times \sin\left(\frac{\hbar k^2}{2M}t\right)Z_{ij}(k,x,y)\right|^2. \quad (3.20)$$

Using the reduced variables

$$\bar{x} = \frac{x}{a}, \quad \bar{y} = \frac{y}{a}, \quad \bar{k} = ak, \quad \bar{K} = aK, \quad \bar{t} = \frac{\hbar}{Ma^2}t, \quad \bar{\beta} = \frac{\hbar^2\beta}{Ma^2}, \quad \bar{u}_0 = \frac{Ma^2}{\hbar^2}u_0, \quad (3.21)$$

we plot in Fig. 3 the average transition-path time as a function of the final point $\bar{y}$ for the initial points $\bar{x} = -4, -2$ (blue dashed line and purple dotted lines, respectively) and the reduced (inverse) temperature $\bar{\beta} = 1$ and barrier height $\bar{u}_0 = 1$. As in the case of the δ-function potential, to the right of the initial point but to the left of the barrier, one notices a reduction of the transition time as the distance increases. The red dash-dotted line is at a reduced (inverse) temperature of $\bar{\beta} = 5$ and initial point $\bar{x} = -4$. Reducing the temperature increases the transit time, as might have been expected.

It is also of interest to study the dependence of the transition time on the reduced barrier height. This is shown in Fig. 4 for $\bar{x} = -\bar{y} = -10, -8, -6-4, -2$ and $\bar{\beta} = 20$. The further away the initial point is from the barrier, the longer the average transit time is. This is reasonable; the differences between the five initial points reflect the longer path in each case. What is more interesting is that in all cases, when the barrier is of order 5 or more, the average transit time becomes almost independent of the barrier height. The Hartman effect is for a barrier with a fixed height but increasing width. We just saw that for a barrier of fixed width but increasing height the mean transit time becomes independent of the barrier height. When the barrier height is low, the average transit time becomes

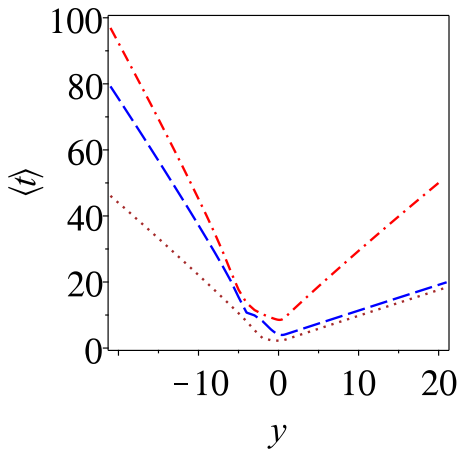

FIG. 3. Mean transition time for a square-barrier potential plotted as a function of the final (reduced) position for a reduced barrier height $\bar{u}_0 = 1$ and the initial points $\bar{x} = -4, -2$ (blue dashed line and purple dotted line, respectively) and a reduced (inverse) temperature $\bar{\beta} = 1$. The red dash-dotted line is with the same conditions but at a reduced (inverse) temperature of $\bar{\beta} = 5$ and initial point $\bar{x} = -4$.

larger, reflecting the fact that for a free particle the average transit time would diverge. As the barrier height increases, tunneling takes over and as mentioned, the average transit time becomes constant when the barrier height is sufficiently large.

Also plotted in Fig. 4 as the dotted lines is the time it would take a classical free particle to cross the distance $2(|\bar{x}| - 1)$ [see Eqs. (3.22) and (3.23) below]. This is the distance to be traversed but excluding the barrier region. The excellent correspondence between this classical estimate and the quantum results as shown in the figure indicates (as will

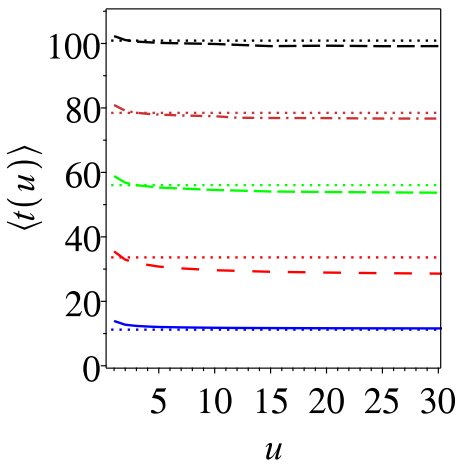

FIG. 4. Mean transition time for a square-barrier potential plotted as a function of the (reduced) barrier height. The reduced (inverse) temperature in all cases is $\bar{\beta} = 20$. The black dashed, purple dash-dotted, green dashed, red dashed, and blue solid lines correspond to the initial positions $\bar{x} = -\bar{y} = -10, -8, -6, -4, -2$, respectively. The dotted lines show the transit time for a classical free particle with the averaged thermal momentum of Eq. (3.22) moving over the distance $2(\bar{y} - 1)$.

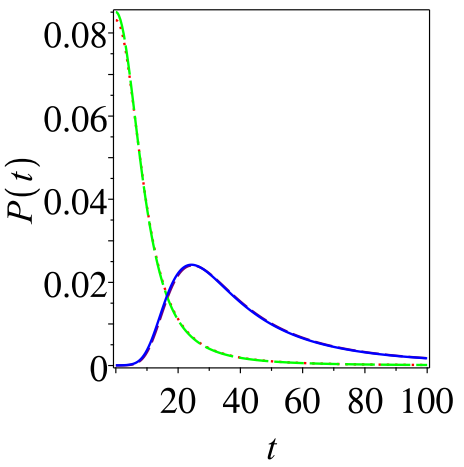

FIG. 5. Mean transition-time probability distribution plotted for a square-barrier potential for two different values of the initial point and the barrier height. The reduced (inverse) temperature in all cases is $\bar{\beta} = 20$. The green long-dashed and red dotted lines are for the initial point $\bar{x} = -2 = -\bar{y}$ and the reduced barrier heights $\bar{u} = 30, 10$ respectively. The blue solid and purple dashed lines are for the initial point $\bar{x} = -6 = -\bar{y}$ and the reduced barrier heights $\bar{u} = 30, 10$, respectively.

also be discussed further below) that the time it takes to cross the barrier, that is, the tunneling time, vanishes.

This independence of the transit time on barrier height is shown in even more detail in Fig. 5, where the transition-time probability distribution is plotted for two different initial values of $\bar{x} = -2, -6 = -\bar{y}$ but in each case for the reduced barrier heights of $\bar{u} = 10, 30$. The distribution peaks at shorter times when $\bar{x} = -2$; however, the $\bar{u} = 10, 30$ distributions are indistinguishable on the scale of the plot.

The independence on the barrier height is further shown in Fig. 6, where the average time is plotted as a function of the initial point $\bar{x} = -\bar{y}$ for $\bar{u} = 5, 30$ as the dashed orange and blue solid lines, respectively. As is evident from the figure, the two results are almost indistinguishable. Plotted also, as the dotted green line, is the time it would take a free particle whose initial momentum is thermally distributed to cross the distance $2(|\bar{x}| - 1)$. The average momentum for the free particle is

$$\langle p \rangle_\beta = \frac{\int_0^\infty dp\, p \exp\left(-\frac{\beta p^2}{2M}\right)}{\int_0^\infty dp \exp\left(-\frac{\beta p^2}{2M}\right)} = \sqrt{\frac{2M}{\pi\beta}}, \tag{3.22}$$

so the mean (reduced) time for the free particle to cross the distance $2(|\bar{x}| - 1)$ would be

$$\bar{t}_\beta = \sqrt{2\pi\bar{\beta}}(|\bar{x}| - 1), \tag{3.23}$$

which is the green dotted line plotted in the figure. When $|\bar{x}| = 1$ this mean time vanishes; it is the time for a free particle to cross the distance from $-\bar{x}$ to $\bar{x}$ assuming that the time it takes to cross the barrier region vanishes. As can be seen from the figure, when one considers the mean transit time at large distances from the barrier, it extrapolates to zero at $\bar{x} = -1$, irrespective of the barrier height. This demonstrates that for

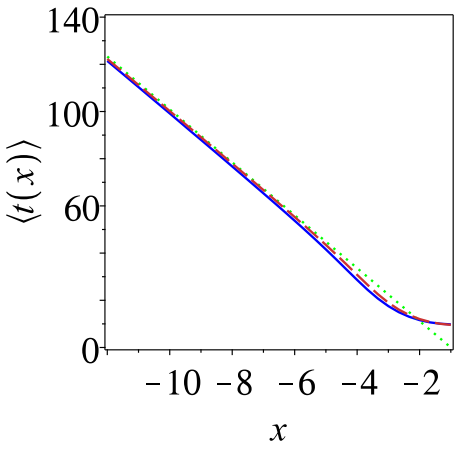

FIG. 6. The transit time through a square barrier vanishes. The mean transition-path time for a square-barrier potential at the reduced temperature $\bar{\beta} = 20$ for the transition path going from x to $-x$ is plotted as a function of the initial (reduced) position (x) for the reduced barrier heights $\bar{u} = 5,30$ as the orange dashed and blue solid lines, respectively. Note that the two lines almost merge. The green dotted line is the time it would take a free particle whose initial momentum is thermally distributed to cross the distance $2(|\bar{x}| - 1)$. At the location of the barrier ($x = -1$) this time vanishes. The quantum transition times extrapolate to this vanishing time, showing that the tunneling time vanishes.

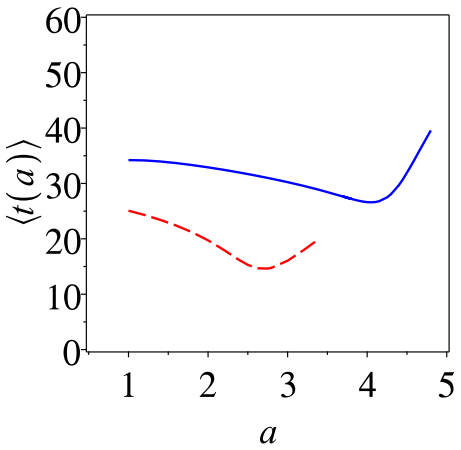

FIG. 7. Thermal Hartman effect. The mean transition time is plotted for a square-barrier potential for two different values of the inverse temperature as a function of the barrier width a. The barrier height $\bar{u} = 1$ is kept fixed at its value for $a = 1$. The mean time is given in terms of the mean time for $a = 1$. The blue solid and red dashed lines are for the inverse temperatures $\bar{\beta}(a = 1) = 20,10$, respectively. For further details see the text.

the square barrier, the time it takes to tunnel through the barrier vanishes.

On the other hand, as the initial point nears the edge of the barrier, the quantum transit time deviates from the classical free-particle estimate and goes to a constant nonzero value at the edge of the barrier ($\bar{x} = -1$). As noted when considering the free particle, the thermal distribution has a spread to it so that at small values of $\bar{x}$ part of the initial distribution is already under the barrier and so does not balance out the longer time it takes the distribution that is on the left side of the initial point to reach the barrier. Considering that the reduced inverse temperature is $\bar{\beta} = 20$, one finds that the standard deviation of the Wigner distribution in configuration space (3.3) is $\sqrt{(\bar{\beta}/4)} \simeq 2.24$, so one would expect that the transit time at $\bar{x} = -1$ would be similar to the transit time at $\bar{x} = -1$ to 2.24, which is roughly the result shown in the figure. However, when the initial point is far from the barrier edge, one obtains a transit time that follows the free-particle classical estimate and is consistent with a vanishing tunneling time.

Finally, it is of interest to study the Hartman effect in the context of thermal tunneling. Since all the variables scale with the width a [see Eq. (3.21)] one has to account for the correct scaling. The results in Fig. 7 are based on their values when $a = 1$. Thus, the barrier height is kept fixed at $\bar{u}(a = 1) = 1$. Similarly, the reduced (inverse) temperature and mean time shown in the figure are based on their value when $a = 1$. The initial and final points are kept at a distance of 3 from the edges of the square barrier, so the free motion part is the same for all values of the width a. The blue solid and red dashed lines are for the inverse temperatures $\bar{\beta}(a = 1) = 20,10$ respectively.

The Hartman effect was discovered for tunneling at a fixed energy. Here we are dealing with an initial thermal distribution. The lower the temperature, the longer the transit time; this is a reflection of the free-particle part of the motion. As the width of the barrier increases, the mean time first decreases and then increases. The initial decrease is a reflection of the Hartman effect. As the barrier becomes thicker, the transmission probability becomes smaller. The higher the incident energy, the more probable it is to tunnel, but the tunneling time is only slightly dependent on the initial energy. Thus, increasing the width increases the contribution from higher incidence energies, which are still below the barrier height. This increases the speed at which the system crosses the free-particle portion to the left and right of the barrier.

For a very thick barrier, the transmission probability goes roughly as [see Eq. (A13)] $\exp(-2aK)$. At some point, the width a becomes so large that the canonical population factor at the barrier energy $\exp(-\beta u_0)$ equals the tunneling exponential. At this point, population moves over the barrier, albeit slowly. This results in the increase of the transit time when the barrier becomes too thick. One notes that the smaller the inverse temperature, the earlier the onset of the increase in the transit time.

The dependence of the transit time on the barrier height and thickness behave quite differently for a thermal initial distribution. Increasing the barrier height decreases the thermal factor $\exp(-\beta u_0)$ exponentially, so there is no contribution from motion above the barrier and the mean tunneling time remains constant. Increasing the width reduces the transmission probability while keeping the thermal factor fixed, so at some point, thermal activation "beats" the tunneling and the transit time again increases with the width.

D. Symmetric double-well potential at very low temperatures

For a symmetric-double-well potential at very low temperatures, one may assume that only the two lowest eigenstates (Φ_0 and Φ_1) of the Hamiltonian are populated. Denoting the respective energies by E_0 and $E_0 + \Delta E$, where ΔE is the usual

tunneling splitting, the thermal propagator may be written as

$$\exp(-i\hat{H}t_c) = \exp\left(-\frac{\beta E_0}{2} - i\frac{E_0 t}{\hbar}\right)\Big[|\Phi_0\rangle\langle\Phi_0| + \exp\left(-\frac{\beta\Delta E}{2} - i\frac{\Delta E t}{\hbar}\right)|\Phi_1\rangle\langle\Phi_1|\Big]. \tag{3.24}$$

Assuming that the eigenfunctions are real, we readily find that

$$\begin{aligned}|\langle x|\exp(-i\hat{H}t_c)|y\rangle|^2 &= \exp(-\beta E_0)\Big[\langle x|\Phi_0\rangle^2\langle\Phi_0|y\rangle^2 + 2\cos\left(\frac{\Delta E t}{\hbar}\right)e^{-\beta/\Delta E2} \\ &\times \langle x|\Phi_0\rangle\langle\Phi_0|y\rangle\langle y|\Phi_1\rangle\langle\Phi_1|x\rangle \\ &\times + e^{-\beta\Delta E}\langle x|\Phi_1\rangle^2\langle\Phi_1|y\rangle^2\Big].\end{aligned} \tag{3.25}$$

The normalization integral may be limited to the period $2\pi\hbar/\Delta E$ and one readily finds that the mean transition time is thus

$$\left\langle t\left(x,y,\tau = \frac{2\pi\hbar}{\Delta E}\right)\right\rangle = \frac{2\pi\hbar}{\Delta E}\frac{[\langle x|\Phi_0\rangle\langle\Phi_0|y\rangle + \exp(-\frac{\beta\Delta E}{2})\langle x|\Phi_1\rangle\langle\Phi_1|y\rangle]^2}{[\langle x|\Phi_0\rangle^2\langle\Phi_0|y\rangle^2 + \exp(-\beta\Delta E)\langle x|\Phi_1\rangle^2\langle\Phi_1|y\rangle^2]}. \tag{3.26}$$

To gain further insight, we assume that the eigenfunctions are Gaussian functions so that

$$\frac{1}{\sqrt{2}}[\langle x|\Phi_0\rangle \pm \langle x|\Phi_1]\rangle = \left(\frac{\Gamma}{\pi}\right)^{1/4}\exp\left(-\frac{(x\pm x_0)^2}{2\Gamma}\right) \tag{3.27}$$

and Γ is a width parameter. Using the reduced time and inverse temperature

$$\bar{t} = \frac{\Delta E}{2\pi\hbar}t, \quad \bar{\beta} = \beta\Delta E, \tag{3.28}$$

we plot in Fig. 8 the mean transit time (with $x_0 = 1$, $\bar{\beta} = 1$, and $\Gamma = 1$) as a function of the distance y for $x = -1.5, -1, -0.5$. Interestingly, one finds that the mean transit time changes; the longer the distance to y, the shorter the mean transit time. Only when $y = 0$ is the (reduced) time identically equal to unity.

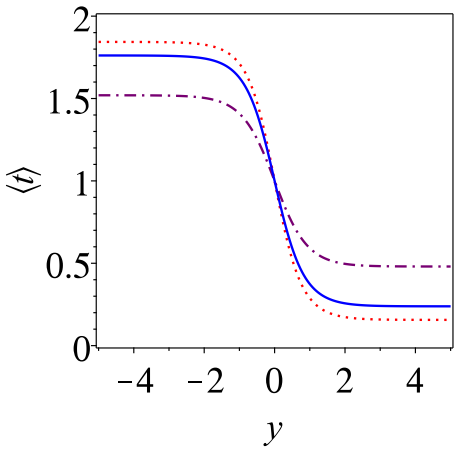

FIG. 8. Mean (reduced) transition time for a symmetric-double-well potential plotted for three different initial points $x = -1.5, -1, -0.5$ as a function of the final point y. The red dotted, blue solid, and brown dash-dotted lines correspond to these three initial conditions. The double-well minima are assumed to be at $x_0 = \pm 1$. Although the time averaged over all final distances is unity, the farther away the distance y and to the right of the initial point, the less time it takes to reach it.

IV. DISCUSSION

The paradigm used in this paper for the study of time is that it should be considered as a parameter in the evolution of quantum-mechanical systems and may be measured through correlation functions. Just as the transit time may be measured in protein folding, it may also be measured in principle when considering any quantum system. A wide class of correlation functions may be constructed that is ensured to be positive and so enable the formulation of a transition-time probability distribution that is well defined.

In this paper the emphasis was on the thermal transit-time distribution for the thermal density correlation function. A system is initially localized around a point in space with a thermal distribution and then measured again when it reaches a different point in the configuration space. In principle, such an experiment is equivalent to a time-of-flight experiment, except that we considered a (positive) thermal density correlation function rather than a thermal flux correlation function [43], which would not be necessarily positive at all times. The positivity was ensured by using a symmetrized thermal initial density; however, the relation between the density correlation function using this symmetrized form and the standard thermal density was considered in some detail. The relationship is one to one, so one may consider the symmetrized thermal density correlation function as being measurable.

The theory was then applied to study the time evolution of a number of simple systems, for which the quantum propagator is known analytically. The first was the free particle from which one may glean two conclusions. One is that for the free particle one cannot construct the transition-time probability distribution, since the time integral of the correlation function diverges at long times. The other is that consideration of the Wigner distribution function of the symmetrized thermal density of the free particle gives insight into the momentum and coordinate spread of the distribution as a function of the temperature.

The first nontrivial system to be analyzed was scattering with a δ-function potential. The most striking result of this system is that the transition-time probability distribution exists even though the particle is almost everywhere a free particle. In other words, the quantum nonlocality is extreme, even arbitrarily far from the center where the δ-function potential is located, the system experiences the potential, and the time evolution is very different from that of a free particle. There is no logarithmic divergence in the time evolution.

The second system studied in some detail was scattering over a square-barrier potential. Qualitative similarities with

the δ-function scattering were noted; however, the dynamics of the square barrier is much richer. We found that, indeed, the mean transit time it takes to tunnel vanishes. This is consistent with the fact that we also demonstrated that the mean transit time is independent of the square-barrier height. On the other hand, with the thermal density distribution one does not find that the mean transit time is independent of the width of the barrier, known as the Hartman effect. For a fixed barrier height, at very low temperature, increasing the barrier width initially shortens the transit time, but at some point the transit time again increases with width. This occurs when the tunneling probability becomes smaller than the probability for above barrier crossing. At longer lengths, the system crosses above the barrier, motion is slow, and the transit time naturally increases.

Finally, the formalism was applied to the dynamics of a symmetric-double-well potential at very low temperature. Just as in the cases of the δ-function and square-barrier potentials, here too there are regions where the longer the distance, the shorter the time it takes to traverse it. Most interestingly, the transit time scale is determined by the standard double-well splitting energy (inversely proportional to it); however, the transit time is not constant; it depends on the distance between the initial and final density.

In contrast to the studies presented in Refs. [31,32], we did not consider the effects of friction. For a parabolic barrier this may be carried out analytically; this is not the case for the systems studied here. Introducing friction to the problem, though very interesting, would necessarily involve numerical studies that are not trivial. Another aspect that has not been considered here is the study of the transit time based on correlation functions that are not thermal. A clear case to be analyzed in detail is when the initial operator is a projection onto a coherent state and the transit is to a final density. This would be the formalism needed to analyze the double-slit experiment, for example, and to obtain not only the diffraction pattern but also its evolution in time.

There are many other quantum effects whose time evolution could be considered using the transit-time probability distribution formalism. Examples are quantum resonances, quantum reflection at low energy, curve crossing problems, and photoinduced transitions. This present study will hopefully stimulate a deep study into the temporal behavior of quantum systems.

ACKNOWLEDGMENTS

I thank Professor J. Richardson for useful discussions. This work was supported by grants of the Minerva Stiftung, Munich, and the Israel Science Foundation.

APPENDIX

In this appendix we summarize the necessary formulas for the propagator of the square-barrier potential as given in Ref. [36]. The function $Z_{ij}(k,x,y)$ appearing in Eq. (3.18) is written as

$$Z_{ij}(k,x,y) = F_s(k)Y_{is}(k,x)Y^*_{js}(k,y) + F_a(k)Y_{ia}(k,x)Y^*_{ja}(k,y), \tag{A1}$$

with

$$F_s(k) = \frac{1}{\pi}\frac{k^2}{k^2|\cosh(Ka)|^2 + |K|^2|\sinh(Ka)|^2}, \tag{A2}$$

$$F_a(k) = \frac{1}{\pi}\frac{k^2}{|K|^2|\cosh(Ka)|^2 + k^2|\sinh(Ka)|^2}, \tag{A3}$$

$$Y_{1s} = \cosh(Ka)\cos[k(x+a)] - \frac{K}{k}\sinh(Ka)\sin[k(x+a)], \tag{A4}$$

$$Y_{0s} = \cosh(Kx), \tag{A5}$$

$$Y_{2s} = \cosh(Ka)\cos[k(x-a)] + \frac{K}{k}\sinh(Ka)\sin[k(x-a)], \tag{A6}$$

$$Y_{1a} = -\sinh(Ka)\cos[k(x+a)] + \frac{K}{k}\cosh(Ka)\sin[k(x+a)], \tag{A7}$$

$$Y_{0a} = \sinh(Kx), \tag{A8}$$

$$Y_{2a} = \sinh(Ka)\cos[k(x-a)] + \frac{K}{k}\cosh(Ka)\sin[k(x-a)]. \tag{A9}$$

Using these formulas and some manipulation, one finds the following more explicit forms:

$$Z_{12}(k,x,y) = \frac{k^2}{\pi}\frac{K^2\cosh(2Ka)\cos[k(x-y)] + \frac{1}{2}kK\left(\frac{K^2}{k^2}-1\right)\sinh(2Ka)\sin[k(y-x)]}{\frac{M^2u_0^2}{\hbar^4}\sinh(2Ka)^2 + \frac{2Mu_0}{\hbar^2}k^2 - k^4}, \tag{A10}$$

$$Z_{10}(k,x,y) = \frac{K^2k^2}{\pi}\frac{\cos[k(x+a)][\cosh(Ka)^3\cosh(Ky) - \sinh(Ka)^3\sinh(Ky)]}{\frac{M^2u_0^2}{\hbar^4}\sinh(2Ka)^2 + \frac{2Mu_0}{\hbar^2}k^2 - k^4}$$

$$+\frac{k}{2\pi}\frac{\sinh(2Ka)\{k^3\cos[k(x+a)]\sinh[K(a-y)]-K^3\sin[k(x+a)]\cosh[K(a-y)]\}}{\frac{M^2u_0^2}{\hbar^4}\sinh(2Ka)^2+\frac{2Mu_0}{\hbar^2}k^2-k^4}$$
$$+\frac{Kk^3}{\pi}\frac{\sin[k(x+a)][\cosh(Ka)^3\sinh(Ky)-\sinh(Ka)^3\cosh(Ky)]}{\frac{M^2u_0^2}{\hbar^4}\sinh(2Ka)^2+\frac{2Mu_0}{\hbar^2}k^2-k^4}, \tag{A11}$$

$$Z_{11}(k,x,y)=\frac{Kk}{4\pi}\frac{(2Kk[1+\cosh^2(2Ka)]\cos[k(x-y)]-(k^2+K^2)\sinh(4Ka)\sin[k(x+y+2a)])}{\frac{M^2u_0^2}{\hbar^4}\sinh(2Ka)^2+\frac{2Mu_0}{\hbar^2}k^2-k^4}$$
$$+\frac{\sinh^2(2Ka)\{k^4\cos[k(x+a)]\cos[k(y+a)]+K^4\sin[k(x+a)]\sin[k(y+a)]\}}{2\pi\left[\frac{M^2u_0^2}{\hbar^4}\sinh(2Ka)^2+\frac{2Mu_0}{\hbar^2}k^2-k^4\right]}. \tag{A12}$$

These are then inserted into the expressions (3.19) and (3.20) to obtain the mean transition-path time. Finally, the transmission coefficient for the square barrier at an incident energy $E=\hbar^2k^2/2M$ is

$$|T|^2=\frac{4E(u_0-E)}{4E(u_0-E)+u_0^2\sinh^2(2Ka)}. \tag{A13}$$

[1] J. Hilgevoord, Stud. Hist. Philos. Mod. Phys. **36**, 29 (2005).
[2] W. Pauli, *Handbuch der Physik* (Springer, Berlin, 1933), Vol. 24, pp. 83–272.
[3] J. G. Muga, R. Sala Mayato, and I. L. Egusquiza, *Time in Quantum Mechanics*, edited by J. G. Muga, R. Sala Mayato, and I. L. Egusquiza, Lecture Notes in Physics Vol. 734 (Springer, Berlin, 2008), pp. 1–30.
[4] *Time in Quantum Mechanics*—Vol. 1, edited by J. G. Muga, R. Sala Mayato, and I. L. Egusquiza, Lecture Notes in Physics Vol. 734 (Springer, Berlin, 2008).
[5] *Time in Quantum Mechanics*—Vol. 2, edited by J. G. Muga, A. Ruschhaupt, and A. del Campo, Lecture Notes in Physics Vol. 789 (Springer, Berlin, 2009).
[6] V. S. Olkhovsky, Adv. Math. Phys. **2009**, 859710 (2009).
[7] V. S. Olkhovsky, Phys. Usp. **54**, 829 (2011).
[8] P. Grossel, Ann. Phys. (NY) **330**, 74 (2013).
[9] E. E. Kolomeitsev and D. N. Voskresensky, J. Phys. G **40**, 113101 (2013).
[10] A. Sanz and S. Miret-Artés, Ann. Phys. (NY) **339**, 11 (2013).
[11] T. Pashby, Stud. Hist. Philos. Mod. Phys. **52**, 24 (2015).
[12] A. S. Landsman and U. Keller, Phys. Rep. **547**, 1 (2015).
[13] J. J. Halliwell, J. Evaeus, J. London, and Y. Malik, Phys. Lett. A **379**, 2445 (2015).
[14] G. Torres-Vega, J. Math. Phys. **57**, 122111 (2016).
[15] P. Bokes, Phys. Rev. A **83**, 032104 (2011).
[16] R. Sala Mayato, D. Alonso, and I. L. Egusquiza, *Time in Quantum Mechanics—Vol. 1* (Ref. [4]), p. 235.
[17] J. G. Muga, S. Brouard, and R. Sala, Phys. Lett. A **167**, 24 (1992).
[18] D. Home, A. K. Pan, and A. Banerjee, J. Phys. A **42**, 165302 (2009).
[19] J. Léon, J. Julve, P. Pitanga, and F. J. de Urries, Phys. Rev. A **61**, 062101 (2000).
[20] K. Maji, C. K. Mondal, and S. P. Bhattacharya, Int. Rev. Phys. Chem. **26**, 647 (2007).
[21] D. H. Kobe and V. C. Aguilera-Navarro, Phys. Rev. A **50**, 933 (1994).
[22] O. del Barco, M. Ortuño, and V. Gasparian, Phys. Rev. A **74**, 032104 (2006).
[23] D. Sokolovski and L. M. Baskin, Phys. Rev. A **36**, 4604 (1987).
[24] D. Sokolovski, *Time in Quantum Mechanics—Vol. 1* (Ref. [4]), p. 195.
[25] G. Hummer, J. Chem. Phys. **120**, 516 (2004).
[26] A. M. Berezhkovskii, G. Hummer, and S. M. Bezrukov, Phys. Rev. Lett. **97**, 020601 (2006).
[27] B. W. Zhang, D. Jasnow, and D. M. Zuckerman, J. Chem. Phys. **126**, 074504 (2007).
[28] S. Chaudhury and D. E. Makarov, J. Chem. Phys. **133**, 034118 (2013).
[29] E. Pollak, Phys. Chem. Chem. Phys. **18**, 28872 (2016).
[30] K. Neupane, D. A. N. Foster, D. R. Dee, H. Yu, F. Wang, and M. T. Woodside, Science **352**, 239 (2016).
[31] E. Pollak, J. Phys. Chem. Lett. **8**, 352 (2017).
[32] E. Pollak, Phys. Rev. Lett. **118**, 070401 (2017).
[33] I. R. Craig and D. E. Manolopoulos, J. Chem. Phys. **121**, 3368 (2004).
[34] B. Gaveau and L. S. Schulman, J. Phys. A: Math. Gen. **19**, 1833 (1986).
[35] M. A. M. de Aguiar, Phys. Rev. A **48**, 2567 (1993).
[36] G. J. Papadopoulos, Task Q. **19**, 65 (2015).
[37] T. E. Hartman, J. Appl. Phys. **33**, 3427 (1962).
[38] H. G. Winful, Phys. Rep. **436**, 1 (2006).
[39] J. T. Lunardi, L. A. Manzoni, A. T. Nystrom, and B. M. Perreault, J. Russ. Las. Res. **32**, 431 (2011).
[40] D. Sokolovski, Proc. R. Soc. London A **460**, 1505 (2004).
[41] A. Ruschhaupt, J. G. Muga, and G. C. Hegerfeldt, *Time in Quantum Mechanics—Vol. 2* (Ref. [5]), p. 65.
[42] R. P. Feynman and A. R. Hibbs, *Quantum Mechanics and Path Integrals* (McGraw-Hill, New York, 1965).
[43] E. Pollak and W. H. Miller, Phys. Rev. Lett. **53**, 115 (1984).